Reliable Deep-Learning based Underwater Optical OFDM Wireless Communications

Zeyad A. H. QASEM
School of Electronic and Computer Engineering
Peking University,
Shenzhen, China
zeyadqasem@pku.edu.cn

Amjad Ali
School of Electronic and Computer Engineering
Peking University,
Shenzhen, China
amjad@pku.edu.cn

Bohua Deng
Tsinghua Shenzhen International Graduate School and Tsinghua-Berkeley Shenzhen Institute,
Tsinghua University
Shenzhen, China
dbh21@mails.tsinghua.edu.cn

Qian Li
School of Electronic and Computer Engineering
Peking University,
Shenzhen, China
liqian@pkusz.edu.cn

H. Y. Fu
Tsinghua Shenzhen International Graduate School and Tsinghua-Berkeley Shenzhen Institute,
Tsinghua University
Shenzhen, China
hyfu@sz.tsinghua.edu.cn

***Abstract*— We propose and demonstrate deep learning-based fast-orthogonal frequency division multiplexing (FOFDM-DL) system for underwater optical wireless communications. FOFDM-DL significantly outperforms the conventional OFDM in terms of peak-to-average power ratio (PAPR), and bit error rate (BER).**

Keywords—OFDM, underwater communications, DL, PAPR and FOFDM.

I. INTRODUCTION

Underwater communication is recently considered as one of most important research fields due to its role in tactical environmental monitoring, marine research and disaster prevention [1]. Compared to other used techniques such as acoustic and radio frequency (RF) waves, underwater optical wireless communications (UOWC) represent a promising option over short-distance communications due to its offered high-rate transmission, cost-effectiveness and low power consumption. On the other hand, underwater channel characteristics that highly absorbs optical signals, and leads to optical scattering limits UOWC performance. Therefore, direct current optical orthogonal frequency division multiplexing (DCO-OFDM) has been adopted to combat the channel effects where Hermitian symmetric (HS) and such DC bias are employed for forcing the transmitted signal to be unipolar and real at the cost of achieved data rate and power efficiency, respectively [2].

Fast-OFDM (FOFDM) [3], which is based on real transforms such as discrete Hartley transform (DHT) or discrete cosine transform (DCT), has been presented to overcome the requirement to HS, but, similar to OFDM, F-OFDM is still suffering from the major drawbacks of the DC bias and high peak-to-average power ratio (PAPR). Those issues become more critical in UOWC system as sustainable energy source is more difficult in that environment and bit error rate (BER) performance is supposed to be worse. It's worth mentioning that DCO-OFDM and/or DCO-FOFDM are still the most efficient systems in term of PAPR and spectral efficiency (SE) compared to their benchmarks which utilize clipping process to avoid the DC bias such as asymmetrically clipped O-OFDM (ACO-OFDM), [4] layered ACO-OFDM (LACO-OFDM) [5] and others.

Several techniques have been proposed to solve the issue of PAPR using precoded OFDM [6] or pilot-based OFDM [7]. The use of precoded OFDM increases the sensitivity non-linear effects making it less attractive to such practical UWOC systems while the pilot-based OFDM limits the SE as pilot symbol must continuously be transmitted. Recently, auto-encoder deep learning-based DCO-OFDM has been found to be an efficient solution to reduce the PAPR [8, 9], but at the cost of huge deterioration of BER as the two parts of auto-encoder must be identical at the transmitting and the receiving ends.

This paper presents a novel deep learning-based FOFDM where a deep learning model is used at the transmitting end to reduce the PAPR effect while another deep learning model is employed at the receiving end for detecting the transmitted data. Both parts are trained to reduce the PAPR and BER effects jointly. Different from those systems in literatures, two deep learning models configuration can be configured independently to produce a satisfied performance. In the proposed system, the idea of vector OFDM (V-OFDM) [10] is also implemented to avoid the degradation of BER performance and, at the same time, improve the achieved data rate by reducing the required guard interval. For instance, the proposed system offers up to 10.5 dB PAPR reduction and 3 dB in term of BER. Moreover, the required DC bias is reduced significantly.

The rest of this paper is structured as follows: section II presents the system model of our proposed FOFDM-DL system. Section III presents the simulation results and discussion, and the conclusion is presented in section IV.

II. SYSTEM MODEL

Fig. 1 shows the model structure of the proposed system. The incoming information bits $\mathcal{B}$ are first modulated using M-ary pulse amplitude modulation (M-PAM); and the modulated data $\boldsymbol{x} \in \mathbb{R}^{N\times 1}$ loaded into N subcarriers to generate the OFDM symbol. For simplicity, let's consider one symbol in our system, and the same process can be implemented for other symbols. Therefore, each symbol is first divided into G vectors with length of each vector of L such that $N = GL$. The data carried by the g-th vector is given by $\boldsymbol{x}_g = \left[x_{gL}, x_{gL+1}, \cdots, x_{gL+L+1}\right]^T$, where $(.)^T$ represents the transpose operation and $g = 0,1,\cdots,G-1$. After that, each

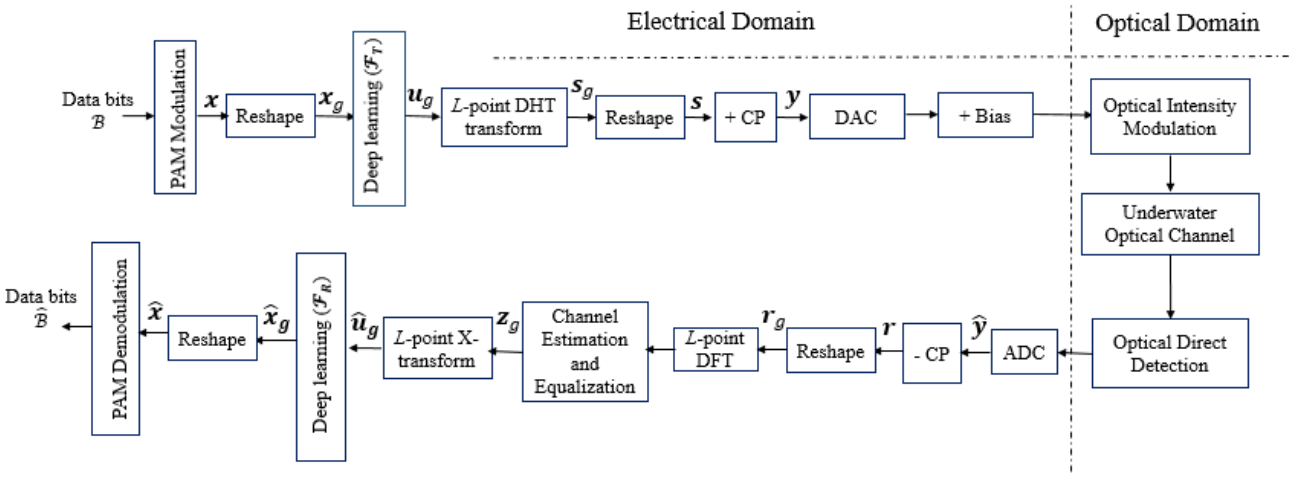

Fig. 1: Structure of FOFDM-DL over underwater optical wireless communications

vector is inserted first to the deep learning model at the transmitting end $\boldsymbol{\mathcal{F}_T}$ resulting its corresponding output $\underline{\boldsymbol{u}}_{\boldsymbol{g}} \in \mathbb{R}^{(L-2)\times 1}$. Particularly, $\underline{\boldsymbol{u}}_{\boldsymbol{g}}$ can be expressed in function of the parameters of first fully connected (FC) layer by $\underline{\boldsymbol{u}}_g = \mathcal{W}_1^a \boldsymbol{x_g} + b_1^a \in \mathbb{R}^{Q\times(L-2)}$, where $\mathcal{W}_1^a$ and b_1^a represent the weights and biases of first FC layer, and Q is the number of hidden nodes. Then, the final output is acquired using tanh activation function as

$$\boldsymbol{u_g^{(1)}} = \mathcal{f}_{tanh}\left(\mathcal{W}_1^a \underline{\boldsymbol{u}}_g + b_1^a\right). \tag{1}$$

Different from the conventional O-OFDM, it's clear the proposed system does not lose data caused by forcing the DC components to be zeros which become severe in case of direct adaptation of V-OFDM into OWC as the number DC components will be increased. In order to ensure the average transmit power per symbol E_s, PowerNorm is applied to get the final output of $\boldsymbol{\mathcal{F}_T}$ as

$$\boldsymbol{u}_g = \frac{\sqrt{E_s}\,\boldsymbol{u}_g^{(1)}}{\sqrt{\mathbb{E}\left[\left\|\boldsymbol{u}_g^{(1)}\right\|^2\right]}}, \tag{2}$$

where $\mathbb{E}[.]$ is the expectation of [.]. So, the time-domain signal of the g-th vector is given by

$$\boldsymbol{s_g} = \boldsymbol{D}\boldsymbol{u_g}, \tag{3}$$

where $\boldsymbol{D} \in \mathbb{R}^{\boldsymbol{L}\times\boldsymbol{L}}$ represented the DHT matrix whose (n,m) -entry is given by $d_{n,m} = cas(\frac{2\pi nm}{L})$, where $cas\left(\frac{2\pi nm}{L}\right) = \cos\left(\frac{2\pi nm}{L}\right) + \sin\left(\frac{2\pi nm}{L}\right)$.

After performing that process from (1) to (3) to all vectors, the resulted data is multiplexed to form the time-domain $\boldsymbol{s} \in \mathbb{R}^{N\times 1}$ vector data. In order to prevent the inter symbol interference (ISI), the cyclic prefix (CP) guard interval is added into the baseband signal $\boldsymbol{s}$. Moreover, well-known training sequences (TS) are added into the beginning of the each frame for synchronization and estimation task. The data is then converted into serial to be transmitted via UOWC channel; the received photocurrent by the photo-detector signal $\boldsymbol{r}$ can be expressed as

$$\boldsymbol{r} = \boldsymbol{h} \oplus \boldsymbol{y} + \boldsymbol{v}, \tag{4}$$

where $\boldsymbol{h}$ is the UOWC channel impulse response, $\oplus$ is circular convolution operation and $\boldsymbol{v}$ the photo-detector responsivity which is normally modeled as an additive white Gaussian noise (AWGN) with zero mean and variance σ^2.

At the reception end, the received signal $\boldsymbol{r}$ is first converted into parallel and each symbol is processed independently. After removing the CP, the convolution between the transmitted signal and channel is circular and every vector can be processed separately using minimum mean square error (MMSE) equalizer [11]. Hence, without the loss of the generality, the data of each vector is forwarded into L-point DFT to perform MMSE equalization as in [11, Eq. 9] yielding $\boldsymbol{z}_g$ and followed by low-complexity matrix multiplication called X-transform similar to our previous work in [12]. Therefore, the estimated signal $\hat{\boldsymbol{u}}_{\boldsymbol{g}}$ is found using low-complexity X-matrix shown in [13] as

$$\hat{\boldsymbol{u}}_{\boldsymbol{g}} = \boldsymbol{X}\boldsymbol{z}_{\boldsymbol{g}}\,. \tag{5}$$

The output of the X-transform is inserted into deep learning at the receiving end $\boldsymbol{\mathcal{F}_R}$ to produce $\hat{\boldsymbol{x}}_g$; and finally the demodulation is processed to recover the transmitted information bits $\hat{\mathcal{B}}$. It's worth mentioning here that processing of $\boldsymbol{\mathcal{F}_R}$ is similar to DNN at the transmitting end with respect to the structure and parameters of $\boldsymbol{\mathcal{F}_R}$.

One of the vital roles in determining the overall OFDM UOWC systems is the PAPR of the output signal. Similar to OFDM, V-OFDM and FOFDM are suffering from high PAPR given by

$$PAPR_{(s)} = \frac{\max\limits_{0\le k\le N-1}\|s_k\|^2}{\text{mean}(\|s_k{}^2\|)}\,. \tag{6}$$

In this work, we seek to solve the issue of PAPR effect without affecting the overall performance of the system. Therefore, deep learning is used at the transmitting and receiving ends to jointly reduce the PAPR in (6) and the BER performance. That deep learning models are trained offline to reduce the system complexity. The channel effects are recovered first to aid the deep learning models to be environment independent; so training process is not required in the test stage despite the UOWC harsh channel which might be time-varied.

A. Training process

To enable the use of deep neural networks (DNN), it needs to be trained offline first. In the training stage, random data is generated using statistic UWOC channel collected using 2-meter pool. The scenario of that process is given as follows: DCO-FOFDM signal is generated, but without the use of DNN; it means the data is modulated and inserted into DHT

matrix. Then, the same process explained above is followed till generating the signal $\boldsymbol{y}$. After that, $\boldsymbol{y}$ is uploaded into the arbitrary waveform generator (AWG071X, Tektronix), with sampling frequency of 1 Gsamples/s, and clipping the output of the AWG with $0.5V_{pp}$. The DC bias was added as 2.4 Voltage before transmitting the signal via red 680-nm vertical cavity surface emitting lasers (VCSEL) with bandwidth of 1.13 GHz. The receiving end contains a lens to focus the signal followed by an avalanche photodiode (APD) module (APD210, Menlo Systems) whose bandwidth is 1 GHz and connected to an oscilloscope (OSC, DPO75902SX, Tektronix). The receiver sampling frequency was set to 12.5 GSamples/s. After collecting the signal and processing it offline, the estimated channel is extracted and used to achieve the training process. Different SNR values are used for the training as shown shortly later.

The training process is done to optimize the difference between $\boldsymbol{x_g}$ and the output $\boldsymbol{\mathcal{F}_R}$. Hence, the relationship between the input of $\boldsymbol{\mathcal{F}_T}$ and the output of $\boldsymbol{\mathcal{F}_R}$ can be expressed as

$$\hat{\boldsymbol{x}}_{\boldsymbol{g}} = \boldsymbol{\mathcal{F}_R}\{\boldsymbol{\Phi}(\boldsymbol{h} \oplus \boldsymbol{D}[\boldsymbol{\mathcal{F}_T}(\boldsymbol{x_g})]) + \boldsymbol{n}\}, \tag{7}$$

where $\boldsymbol{\Phi}$ is the equalization operation explained earlier.

The deep learning is trained end-to-end to minimize both the loss functions of BER (ζ_1) and PAPR effects (ζ_2) given by

$$\zeta_1(\theta) = \frac{1}{T}\sum_{i=0}^{T-1}\left\|x_{i,g} - \hat{x}_{i,g}\right\|^2 \tag{8A}$$

$$\zeta_2(\theta) = PAPR_{(s)} \tag{8B}$$

In (8B), the effect of PAPR is shown in (6), T is the used batch size and θ indicates the parameters of $\boldsymbol{\mathcal{F}_T}$ and $\boldsymbol{\mathcal{F}_R}$ including weights and biases. Therefore, the total loss function used to be optimized is given by:

$$\zeta(\theta) = \lambda_1\,\zeta_1(\theta) + \lambda_2\,\zeta_2(\theta), \tag{9}$$

where λ is the loss scaling factor which adjust the strike of each loss function. The advanced stochastic gradient descent (SGD) method terms as adaptive moment estimation (Adam) is adopted for updating the model parameters θ as:

$$\theta := \theta - \eta\nabla\zeta(\theta). \tag{10}$$

In (10), η and ∇ represent the learning rate and gradient of $\zeta(\theta)$ with respected to θ.

Therefore, the deep learning model is trained offline to optimize $\zeta(\theta)$ and then adopted for online test stage.

B. Online Deployment

The output of training stage are represented by the optimized parameters θ of both $\boldsymbol{\mathcal{F}_T}$ and $\boldsymbol{\mathcal{F}_R}$. These parameters are used to perform the offline testing stage. Therefore, the equalized received signal is put in the DNN to estimate the transmitted modulated data. The pre-processing of equalization makes the received data less sensitive into the environment effects. Therefore, no more training for the DNN is required.

III. Simulation Results and Discussion

In this section, the performance of the proposed system is investigated using the parameters of DNN shown in Table 1. Both AWGN and measured UOWC channels are used to demonstrate the outperformance of our proposed systems in comparison with conventional DCO-OFDM [14], DCO-FOFDM [15] and precoded DCO-FOFDM [6] in terms of PAPR, BER and optimal required DC bias. Walsh matrix was used as a precoder to yield precoded DCO-FOFDM.

Table 1: Structure Parameters of $\boldsymbol{\mathcal{F}_T}$ and $\boldsymbol{\mathcal{F}_R}$

Parameter	DNN ($\boldsymbol{\mathcal{F}_T}$)	DNN ($\boldsymbol{\mathcal{F}_R}$)
Input size	*L*	*L-2*
Output size	*L-2*	*L*
Hidden layers	1	2
Size of hidden layer	128	256-128
Output activation	tanh	relu
Training data size	10^5	
Test data size	10^5	
Loss scale factor (λ_1)	0.001	
Loss scale factor (λ_2)	0.001	
Learning rate (η)	0.001	
Batch size (T)	10^3	

We consider $N = 256$, 4-QAM modulation order for DCO-OFDM and 2PAM for both DCO-FODM, and the proposed FOFDM-DL, CP = 32, and the number of vectors $L = 32$ with proposed system. The SNR used for the training of FOFDM-DL is set to 10 dB. So, Fig. 2 shows the CCDF the PAPR performance. It's clear that our proposed system offers up to 10.5 dB better PAPR performance compared to conventional DCO-OFDM and DCO-FOFDM and 9 dB compared to the precoded FOFDM with only one hidden layers at $\boldsymbol{\mathcal{F}_T}$ whose size is 128. That reduction is coming from the use of real modulation order with DNN making it feasible to jointly reduce PAPR and BER.

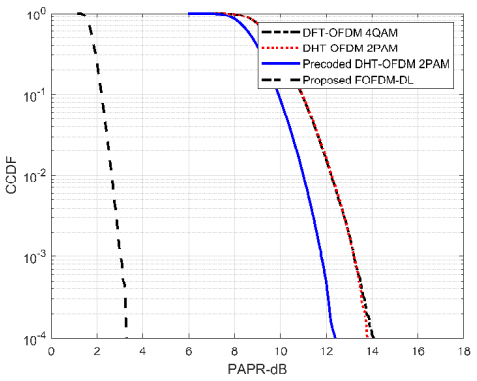

Fig. 2: PAPR performance comparison

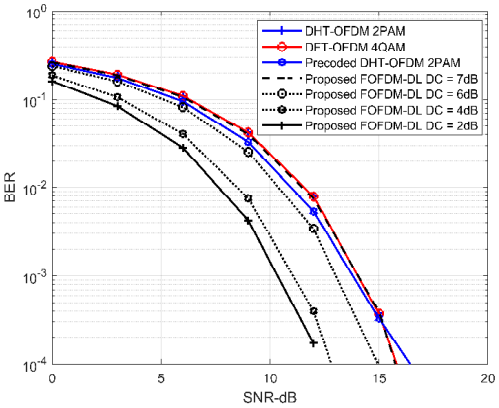

Fig. 3: BER performance comparison over AWGN channel

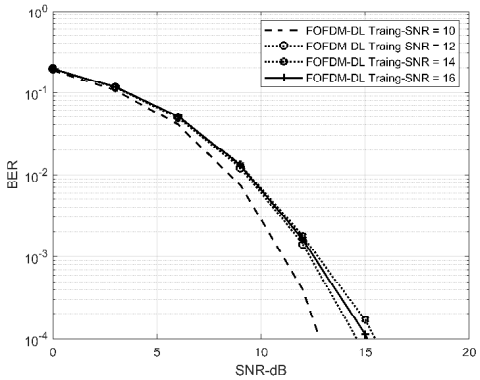

Fig. 4: BER performance at different SNR training levels and DC of 4dB.

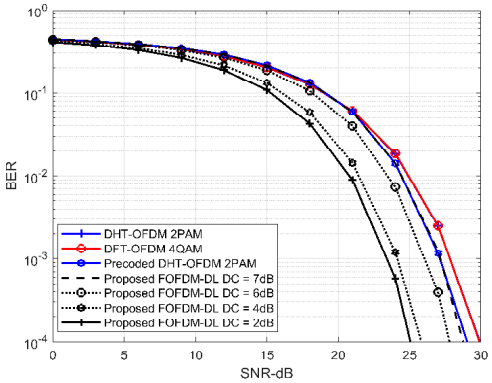

Fig. 5: BER performance over UOWC channel.

Fig. 3 shows the effect of increasing the DC bias on the BER performance; AWGN channel was utilized in that comparison. FODM-DL can significantly improve the power efficiency since it only requires 2 dB DC bias to provide the satisfied performance. Therefore, it can be seen that only 2 dB is required to avoid the clipping effects caused by the nature of optical waves. That outperformance is coming from the training stage which is done without adding any DC bias enabling the DNN to recover the signal even with such clipping effects. It also shown in Fig. 3 that, increasing the added DC bias leads to worse BER performance which is caused by the noise power. Generally, different levels of used training SNR can provide different levels of performance; Fig. 4 shows the performance of BER when setting different levels to the used training SNR. It can be seen and 10 dB provides better performance compared to others.

Finally, Fig. 5 demonstrates the outperformance of FOFDM-DL compared to currently used schemes over measured UOWC channel. The estimation task was performed via the well-known TS, and the equalization operation is performed as explained above. Although, the PAPR was reduced significantly, and the only fewer hidden layers are used at the transmitting and received end, the proposed scheme also provides better performance in term of BER making it a potential alternative solution to the conventional schemes.

IV. Conclusion

In this paper, we presented a novel deep learning-based FOFDM for underwater optical wireless communications. Different from conventional schemes, the proposed scheme employs different DNNs at the transmitting and receiving ends to jointly optimize the PAPR and BER effects. Based on the performance results using both AWGN and UOWC channels, our proposed schemes offer up to 10.5 dB reduced PAPR, 3 dB better BER and higher power efficiency compared to the currently used schemes. In future work, the FOFDM-DL will be proposed with successive interference cancellation in the hybrid orthogonal and non-orthogonal multiple access schemes.

ACKNOWLEDGMENT

Shenzhen Science and Technology Innovation Commission (GXWD20201231165807007-20200827130534001)

REFERNCES

[1] H. Kaushal and G. Kaddoum, "Underwater optical wireless communication," *IEEE access*, vol. 4, pp. 1518-1547, 2016.

[2] Z. Wei, Z. Wang, Q. Li, J. Zhang, and H. Fu, "Evolution of optical wireless communication for B5G/6G," *Progress in Quantum Electronics*, p. 100398, 2022.

[3] A. W. Azim, M. Chafii, Y. Le Guennec, and L. Ros, "Spectral and energy efficient fast-OFDM with index modulation for optical wireless systems," *IEEE Communications Letters*, vol. 24, no. 8, pp. 1771-1774, 2020.

[4] S. Hessien, S. C. Tokgöz, N. Anous, A. Boyacı, M. Abdallah, and K. A. Qaraqe, "Experimental evaluation of OFDM-based underwater visible light communication system," *IEEE Photonics Journal*, vol. 10, no. 5, pp. 1-13, 2018.

[5] R. Bai, S. Hranilovic, Z. Wang, and Networking, "Low-Complexity Layered ACO-OFDM for Power-Efficient Visible Light Communications," *IEEE Transactions on Green Communications*, pp. 1 - 1, 2022.

[6] M. Chen, L. Wang, D. Xi, L. Zhang, H. Zhou, and Q. Chen, "Comparison of different precoding techniques for unbalanced impairments compensation in short-reach DMT transmission systems," *Journal of Lightwave technology*, vol. 38, no. 22, pp. 6202-6213, 2020.

[7] H. T. Alrakah, T. Z. Gutema, S. Sinanovic, and W. O. Popoola, "PAPR Reduction in DCO-OFDM Based WDM VLC," Journal of Lightwave Technology, vol. 40, no. 19, pp. 6359-6365, 2022.

[8] L. Shi et al., "PAPR reduction based on deep autoencoder for VLC DCO-OFDM system," *in 2019 IEEE International Symposium on Broadband Multimedia Systems and Broadcasting (BMSB),* 2019, pp. 1-4: IEEE.

[9] A. Mohamed, A. S. Eldien, M. M. Fouda, and R. S. J. I. A. Saad, "LSTM-Autoencoder Deep Learning Technique for PAPR Reduction in Visible Light Communication," *IEEE Access,* vol. 10, pp. 113028-113034, 2022.

[10] B. Adebisi, K. M. Rabie, A. Ikpehai, C. Soltanpur, and A. Wells, "Vector OFDM transmission over non-Gaussian power line communication channels," *IEEE Systems Journal*, vol. 12, no. 3, pp. 2344-2352, 2017.

[11] Y. Li, I. Ngebani, X.-G. Xia, and A. Host-Madsen, "On performance of vector OFDM with linear receivers," *IEEE Transactions on Signal Processing*, vol. 60, no. 10, pp. 5268-5280, 2012.

[12] Z. A. H. Qasem et al., "Real Signal DHT-OFDM With Index Modulation for Underwater Acoustic Communication," *IEEE Journal of Oceanic Engineering*, pp. 1-14, 2022.

[13] Z. A. Qasem, H. A. Leftah, H. Sun, J. Qi, and H. Esmaiel, "X-Transform Time-Domain Synchronous IM-OFDM-SS for Underwater Acoustic Communication," *IEEE Systems Journal*, pp. 1-12, 2021.

[14] R. Yang et al., "Spectral and Energy Efficiency of DCO-OFDM in Visible Light Communication Systems with Finite-Alphabet Inputs," *IEEE Transactions on Wireless Communications*, pp. 1 - 1 2022.

[15] M. S. Moreolo, R. Muñoz, and G. Junyent, "Novel power efficient optical OFDM based on Hartley transform for intensity-modulated direct-detection systems," *Journal of Lightwave Technology*, vol. 28, no. 5, pp. 798-805, 2010.